

Experimental and theoretical study of magneto-inductive waves supported by one-dimensional arrays of “swiss rolls”

M. C. K. Wiltshire^{a)}

Robert Steiner MRI Unit, Imaging Sciences Department, Imperial College London, Hammersmith Hospital, Du Cane Road, London W12 0NN, United Kingdom

E. Shamonina

Department of Physics, University of Osnabrück, D-49076 Osnabrück, Germany

I. R. Young

Robert Steiner MRI Unit, Imaging Science Department, Imperial College London, Hammersmith Hospital, Du Cane Road, London W12 0NN, United Kingdom

L. Solymar

Department of Engineering Science, University of Oxford, Parks Road, Oxford OX1 3PJ, United Kingdom

(Received 6 August 2003; accepted 26 January 2004)

The propagation of magneto-inductive waves in a one-dimensional array of “swiss roll” metamaterial has been studied. It was found that long-range interactions over the whole of the array must be included to describe the excitations accurately. Using the dispersion relations deduced from experimental data on pairs of elements, the coupling coefficients between all the elements in the array have been determined by matching the experimental and theoretical curves. The relative amplitudes and phases of the excitations on each element in a 31-member array have been measured and compared with the theoretical prediction based on the previously derived coupling coefficients. Excellent agreement between the predicted and measured behavior is found, provided that a full set of coupling coefficients is used. © 2004 American Institute of Physics.
[DOI: 10.1063/1.1687036]

I. INTRODUCTION

It has long been known¹ that the dielectric properties of an insulator can be changed by incorporating variously shaped metallic structures (for example, rods, spheres, disks) within it. These changes are usually modest at microwave frequencies, but can be quite significant at optical frequencies. More recently, Pendry and co-workers showed^{2,3} that radical changes can be obtained, not just in the dielectric properties, but also in the magnetic characteristics of a material, provided that the inclusions have a resonant character. Such materials are known as metamaterials, and can be designed to be active in the rf and microwave frequency ranges (typically 1 MHz to 100 GHz). The magnetic activity occurs in a frequency range which is related to (but is not identical to) the resonant bandwidth of the elements. Finite losses reduce the magnitude of the changes in permeability, but substantial effects can still be obtained with practically achievable materials. When both the permittivity and the permeability are made negative, the refractive index of the material can be regarded as negative (as shown by Veselago in 1968)⁴ leading to some unique properties, e.g., an inverted Snell's law,⁵ and a transverse electromagnetic wave propagation in which the phase and group velocities are in opposite directions.

The resonant elements proposed in Ref. 3 for changing the metamaterial permeability were the split ring resonator

and the swiss roll (essentially a capacitor rolled on a dielectric core as shown in Fig. 1). Experiments with extended swiss roll structures^{6,7} comprised of up to 271 elements, showed that the resulting metamaterial had a high permeability capable of guiding magnetic flux with potential applications in, for example, magnetic resonance imaging.

A third metamaterial element, a capacitively loaded loop, was proposed in Ref. 8. It was pointed out there, using an array of such loops as an example, that a magneto-inductive (MI) wave, due to the magnetic coupling between the elements, may also be excited by an input rf magnetic field. The band of frequencies for which these MI waves can propagate depends on this inter-element coupling: the higher the coupling, the wider the frequency band. The type of the wave, whether forward or backward, was shown to depend on the orientation of the loops. The properties of these waves were studied in more detail in Ref. 9 and were proven experimentally for the one-dimensional (1D) case in Ref. 10. The question then arises: Could the other types of elements, proposed for magnetic metamaterials, also support MI waves? Swiss rolls are obvious candidates since, in any array, the magnetic field generated by one swiss roll is bound to induce currents in other swiss rolls of the array. The aim of the present article is to conduct a detailed experimental and theoretical study showing the existence of MI waves in a 1D array of swiss rolls.

We first consider the choice of the experiments based on theoretical considerations; this is discussed in Sec. II. The experimental setup and the method of measurements are de-

^{a)}Electronic mail: michael.wiltshire@imperial.ac.uk

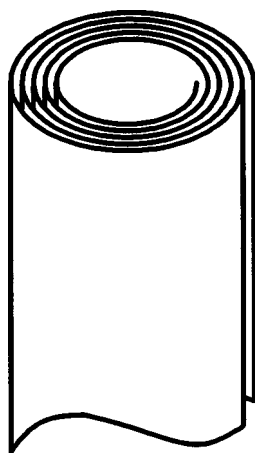


FIG. 1. Schematic representation of a swiss roll, showing the conductor/dielectric laminate wound in a spiral on a central mandrel. When an alternating magnetic field is applied along the axis of the structure, it induces currents in the spiral. Distributed capacitance in the structure allows the currents to flow.

scribed in Sec. III. The experimental results are presented and compared with theory in Sec. IV. Our conclusions are drawn in Sec. V.

II. DETERMINATION OF THE COUPLING COEFFICIENTS

In our previous work,¹⁰ that examined the propagation of MI waves along a 1D array of capacitively loaded loops, the comparison between theory and experiment was fairly straightforward, because only nearest-neighbor interactions needed to be considered. It is more difficult to make the comparison in the present case because higher-order coupling is more significant for swiss rolls. They differ from loops by having a third dimension as well. In the present case, the aspect ratio (length/diameter) of the swiss rolls is about 5. Hence, the magnetic field distribution generated by the swiss rolls is quite different from that of loops: the decline of the magnetic field along the axis of the array is much slower. This has been well known for a long time in the related field of solenoids. The influence of the length of the solenoid on the mutual inductance between two identical solenoids a certain distance apart was studied in detail by those interested in circuit design. For detailed calculations, see Ref. 11.

The consequence of the magnetic field decaying slowly away from each of the elements is that the change of phase and amplitude along the line cannot be described by nearest-neighbor coupling alone. Direct coupling between element 0 and element s , a distance $s \cdot d$ away (where d is the distance between the centers of neighboring elements) may also be important. Such coupling will be referred to as s -order coupling (note that in this terminology nearest-neighbor coupling appears as first-order coupling).

Is there a way of directly measuring higher-order coupling? Fortunately, there is. It can be deduced from a set of “pair” measurements in which the array consists of two elements only at a distance D from each other; the first element is excited and the relative currents in elements 0 and 1 are

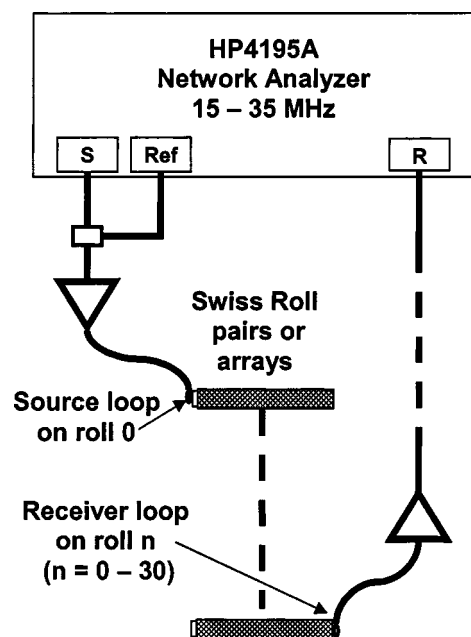


FIG. 2. Schematic of experimental layout. The HP4195A network analyzer drives the 3 mm diameter source loop placed on roll 0. The 3 mm diameter receiver loop detects the flux emerging from the end of the target roll. The rolls are configured either as just a pair or as an array.

measured by probes as shown in Fig. 2. The ratio between these two currents turns out to contain all the information needed. The relationship can be easily derived from the theory presented in Refs. 8 and 9 as

$$I_0/I_1 = 2 \cosh((\alpha + jk)D), \quad (1)$$

where k is the wave number, α is the attenuation coefficient, and $j = \sqrt{-1}$. Since the currents differ from each other both in phase and amplitude, Eq. (1) is sufficient to determine both k and α . Note that in the absence of losses, the two currents represent two points in a pure standing wave, so they must be either in phase or in antiphase. If the currents are measured for a range of frequencies, then we can plot k and α as a function of frequency, and these are none other than the dispersion characteristics. The theoretical dispersion characteristic contains three free parameters: the resonant frequency ω_0 , the quality factor Q , and the coupling constant κ . Out of these three, the resonant frequency and the quality factor can be determined (see Sec. III) by measurements on an individual element, so that only the coupling constant κ remains as a free parameter which can be determined by matching the experimentally obtained dispersion curve to the theoretical one. If in this pair experiment $D = d$, then we measure the first-order coupling coefficient. If $D = sd$, we measure the s -order coupling. Thus, a series of experiments measuring pairs with increasing spacing will allow us to determine the coupling constants κ for each order in turn. These parameters can then be used to derive the behavior of arrays of rolls, all spaced uniformly apart.

III. EXPERIMENTAL SETUP AND MEASUREMENTS

The individual swiss rolls are resonant elements comprised of a spiral of insulated conducting foil tightly wound

on a central mandrel. For optimum performance, both the conductor and the insulating dielectric layer are required to be as thin as possible, with no lossy glue layer between them. Espanex SC18-12-00FR¹² was selected as the most suitable available laminate: This consists of 12 μm of polyimide and 18 μm of copper. the dielectric has a loss tangent of ~ 0.015 at 10 MHz. 50 mm wide strips of this material were wound onto 10 mm diameter acetal mandrels (Fig. 1). 11 turns of laminate gave an overall diameter of 12 mm and a suitable resonant frequency. However, because the rolls were hand made, there was a distribution of resonant frequency that was broader than the width of any individual resonance. The individual rolls were, therefore, tuned using a 40 mm wide, capacitively coupled, Espanex sleeve. This protruded by 10 mm so that the roll and sleeve together were 60 mm long, and the sleeve length was adjusted so that the combination of roll and sleeve had a resonant frequency $f_0 = 21.9 \pm 0.1$ MHz and $Q \sim 65$. A total of 300 rolls were made;⁷ of these, 31 were selected for the present work that had resonant frequencies within a 25 kHz spread.

Two sets of experiments were carried out. In both cases, the measurements were made using an HP4195A network analyzer, with 3 mm diameter loops as both the source and the receiver. Low-noise preamplifiers were used to ensure that the measured signal was well above the noise floor of the system (≤ 100 dB).

In the first set of experiments, we investigated the coupling between a pair of rolls as a function of their separation, from the nearest neighbor up to 30th neighbor. The rolls were placed on a polystyrene foam bed with indentations to maintain the correct positions. One roll was excited by placing the source loop adjacent to the protruding mandrel, about 3 mm away from the end of the Espanex spiral. The detector was placed first at the other end of the excited roll, and then at the end of the second roll. The transmitted amplitude and phase at each position were recorded at 401 frequency points in the range of 15–35 MHz, as a function of roll separation (see Fig. 2).

The 31 rolls were then laid side-by-side so that their center-to-center spacing was 12 mm. Once again, the first roll was excited with the 3 mm diameter source loop, and the transmitted amplitude and phase were recorded at 401 frequency points in the range of 15–35 MHz by placing the 3 mm diameter receiver loop at each roll in the array in turn (see Fig. 2).

IV. COMPARISON BETWEEN THEORY AND EXPERIMENTS

A. Derivation of coupling parameters

As mentioned in the previous Section, 30 pair measurements altogether were conducted, each one of them for 401 values of frequency. In order to find the dispersion relationships, all we need to do is to invert Eq. (1) which will yield both kD and αD as a function of frequency. Conventionally, we plot ω against kD or αD , and the ω versus αD curves obtained this way are shown as dots in Fig. 3(a) for selected pair distances between $D=d$ and $30d$. The attenuation increases steadily with distance, but after the first-neighbor

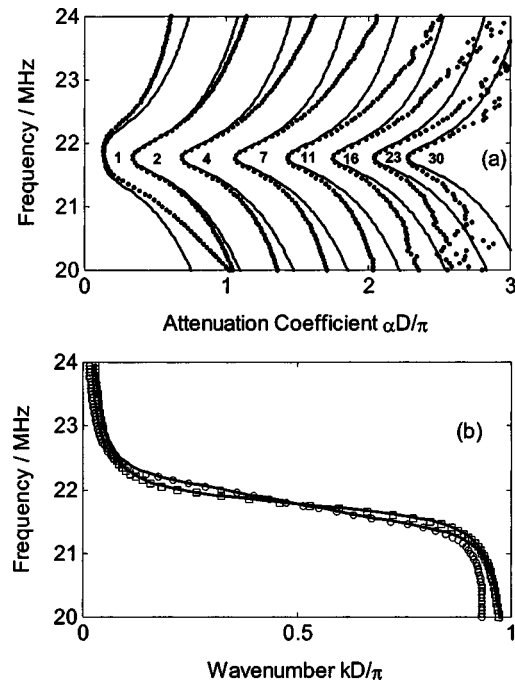


FIG. 3. (a) The frequency variation of the attenuation coefficient derived from the pair measurements for a number of selected distances. The dots are values derived from experimental results, whereas the lines are the theoretical curves based on Eq. (1) using the best fitting coupling coefficients κ . (b) The frequency variation of the wave number or propagation coefficient. The symbols (the circles for nearest-neighbor spacing, squares for second- and further-neighbor spacing) are derived from the experiments; the line from the theoretical description.

case, the curves all retain the same shape and the minimum attenuation occurs at the approximately the same frequency.

The ω versus kD curves may be derived in a similar way. They are shown by circles and squares in Fig. 3(b) for $D=d$ and $2d$, respectively. For larger pair distances all the way up to $D=30d$, the curves coincide.

The theory used closely follows that for loops developed in Refs. 8 and 9. The array of loops was regarded there as a set of coupled resonant circuits and the dispersion characteristics were derived from that assumption. The only difference with regard to swiss rolls is that the coupling coefficients will be different. We may then write the dispersion equation for the pair experiment (only one single coupling coefficient) as^{8,9}

$$I_0/I_1 = 2/\kappa(\omega_0^2/\omega^2 - 1 + j/Q). \quad (2)$$

There are three free parameters in this equation: the resonant frequency ω_0 , the quality factor Q , and the coupling constant κ . Since it has already been established that swiss rolls are resonant structures, and their resonant frequency and quality factor have been determined as 21.9 MHz and 65, respectively, that leaves only one free parameter, the coupling constant. By matching each of the experimental curves (dots) in Fig. 3(a) by a theoretical one (solid lines), the corresponding coupling coefficient can be determined. The match may be seen to be very good near to the resonant frequency but there is some divergence toward the edges of

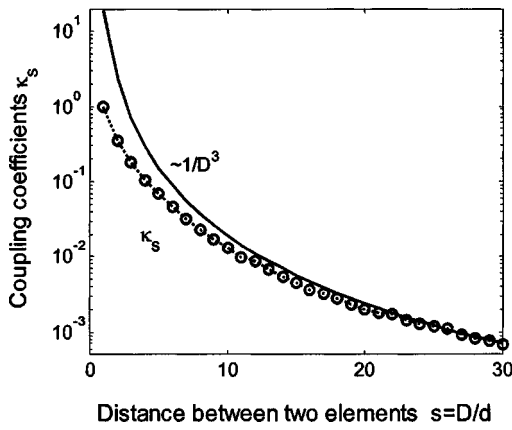


FIG. 4. The values of the 30 coupling coefficients derived from the pair measurements (circles). The dotted line is a guide for the eyes. The full line shows the inverse cube relationship, normalized to the 30th coefficient.

the band. Considering that the model is a very simple one, the overall agreement between theory and experiment may be regarded as good.

The kD versus ω curves found experimentally may also be matched by theoretical ones as shown in Fig. 3(b) by lines for $D=d$ and $2d$. For larger distances, the theoretical curves, as well as the experimental curves, coincide. The reason for this is that, once losses dominate, the kD versus ω curves become independent of the coupling coefficient. Under the assumption of high attenuation the relationship between ω and kD can be easily obtained from Eqs. (1) and (2) in the simple form

$$\omega^2/\omega_0^2 = Q \tan(kd) / (Q \tan(kd) - 1), \quad (3)$$

which is clearly independent of the coupling coefficient.

The coupling coefficients determined by the matching technique are shown in Fig. 4 by a set of circles. As expected, the higher the order of the coupling, the smaller the coupling coefficient. Note that, if the distance between the two elements is large enough, the decay of the coupling coefficient should be proportional to the cube of the distance. This is because, when observed from a sufficiently large distance, a swiss roll (or a solenoid) appears as an infinitely small magnetic dipole. The magnetic field in the vicinity of the swiss roll, as discussed in Sec. II, declines much more slowly due to the finite length of the element. The dotted curve in Fig. 4 shows the cubic decline relative to the last coupling coefficient. It can be clearly seen that the cubic law starts to become valid at around the 24th element. The curves shown in Fig. 4 give an indication of the significance of higher-order coupling.

B. Investigation of array behavior

So far the theory has been quite successful in matching the pair experimental results, but the real test comes when we wish to match the experimental results obtained by measuring the phase and amplitude of the current on each of the elements in a 31-element long array of swiss rolls. We derive the current by inverting the $\mathbf{V}=\mathbf{Z}\mathbf{I}$ relationship^{8,9} where

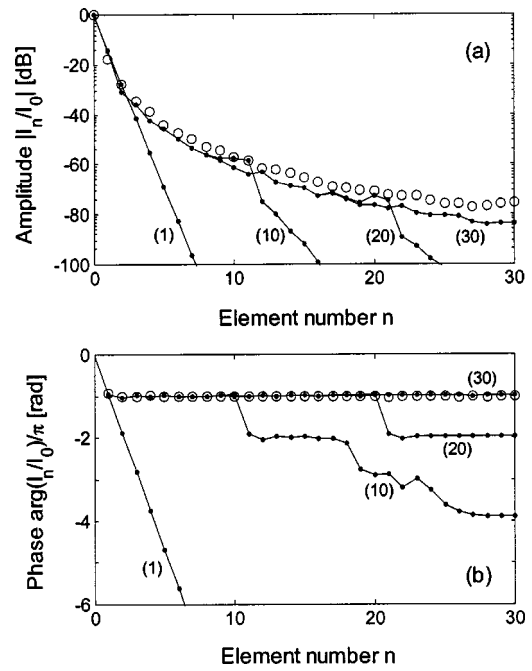


FIG. 5. Amplitude and phase variation along the array at 21.0 MHz. The circles are experimental values, and the lines show the theoretical values when up to 1, 10, 20, and 30 coupling coefficients are taken into account.

$$\mathbf{V} = (1, 0, 0, \dots, 0), \quad (4)$$

because only the first element is excited. The impedance matrix, \mathbf{Z} , is of the form

$$\mathbf{Z} = \begin{bmatrix} Z_0 & j\omega M_{0,1} & \cdots & j\omega M_{0,30} \\ j\omega M_{1,0} & Z_0 & \cdots & j\omega M_{1,30} \\ \vdots & \vdots & \ddots & \vdots \\ j\omega M_{30,0} & j\omega M_{30,1} & \cdots & Z_0 \end{bmatrix}, \quad (5)$$

where $Z_0 = j\omega L + 1/j\omega C + R$, where L , C , and R are the inductance, capacitance, and resistance, respectively, of the individual swiss rolls (all assumed to be identical), and $M_{m,n}$ is the mutual inductance between element m and element n . The mutual inductance is related to the coupling coefficients as

$$2M_{m,n}/L = \kappa_{m-n}. \quad (6)$$

Therefore, once we have determined all the coupling coefficients, we have also found the values of all the mutual inductances.

We have a matrix of 31×31 elements in which each of the off-diagonal elements was determined by the pair experiment. We invert this matrix, and postmultiply it by the transpose of \mathbf{V} to obtain the 31 complex values for the currents in the 31 elements. The test of the model is then that these values (which we shall call the theoretical ones) should agree with the results of the experiment in which the current is measured for each of the elements of the 31-element array. Ideally, the agreement should be close for all 401 values of frequency. Clearly, if we are to hope for any agreement between theory and experiment, the pair measurements have to

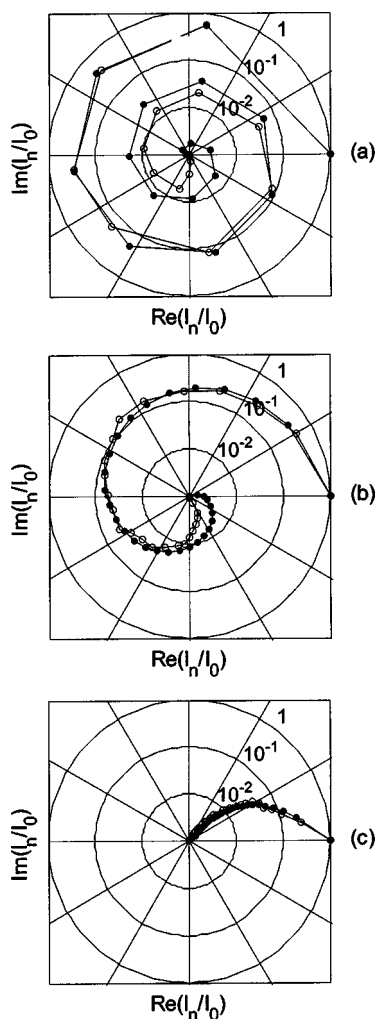


FIG. 6. Complex amplitude of currents along the array, normalized to that at element zero, at (a) 22.0 MHz, (b) 22.5 MHz, and (c) 23.0 MHz. The experimental points are denoted by open circles, the theory by filled circles.

be of very high accuracy and the theoretical model has to be accurate enough to yield the right coupling coefficients.

Figures 5 and 6 show the comparisons with the experimental results. Let us first take a frequency, $f=21.0$ MHz, below the resonance. The measured phase and amplitude of the currents at each element, normalized to the first one in the array, are shown by circles in Figs. 5(a) and 5(b). There are four theoretical curves plotted, taking into account up to 1, 10, 20, and 30 coupling coefficients, respectively. The remarkable conclusion, which applies both to the phase and amplitude, is that a theory taking into account the first 10 coupling coefficients can only match the experiments for the first 11 elements. With 20 coupling coefficients, one can achieve matching for 21 elements; in order to be able to match the results for all the 31 elements, all 30 coupling coefficients are required. It can be regarded as a real triumph of both the theoretical model and of the accuracy of the experiments that we have good agreement in amplitude over a range of 80 dB. It turns out the agreement is not quite as good when the phase variation along the array is faster. We shall, therefore, restrict the comparison to a range of 60 dB in amplitude and, for simplicity, we shall show the results in

the complex plane (note that the radial coordinate is on a logarithmic scale covering three orders of magnitude). The experimental (open circles) and theoretical (filled circles) results are shown in Figs. 6(a)–6(c) for $f=22$, 22.5, and 23 MHz, respectively. In each case, we have good quantitative agreement. Note that the phase progression with frequency in these plots shows a backward wave behavior.

V. CONCLUSIONS

We have investigated the magneto-inductive wave excitations running along 1D arrays of swiss rolls. These waves are governed by the coupling between the elements of the array, i.e., the mutual inductance between various pairs of rolls. Unlike our previous study, when the elements were resonant loops and nearest-neighbor coupling sufficed to provide a good description, we find here that long-range interactions have to be included. A separate experiment, involving only two elements, was performed in order to derive the coupling coefficient between any two elements of the array. We find that these coefficients fall off quite slowly as a function of distance, only tending asymptotically to inverse cube behavior for >24 th-neighbor spacing. The key point here is that the rolls are extended resonators, and only at large separation is the point dipole behavior recovered. This, of course, is well known from the mutual inductance of finite solenoids.¹¹

The theoretical treatment of the arrays is based on a model^{8,9} in which the swiss rolls are regarded as coupled resonators, using the coupling coefficients derived above. A comparison of the theoretical and experimental results has shown good agreement across the whole frequency range of interest (results are plotted at 21, 22, 22.5, and 23 MHz) and for amplitude changes covering a range of about 60 dB.

A remarkable feature of the array, in contrast to any other array we have come across, is the relevance of the higher-order coupling between the elements which is due to the fact that the magnetic field generated by a swiss roll decays relatively slowly away from the element. It has been shown that for determining the complex current in a 31-element array, none of the 30 coupling coefficients can be disregarded.

In conclusion, we have shown that, provided the correct set of coupling coefficients is used, the MI wave formalism accurately describes the propagation of an rf excitation along an array of swiss roll elements.

ACKNOWLEDGMENTS

The authors are grateful to John Cobb for making the “swiss rolls” and to Stephen Wiltshire for assistance with tuning them and constructing the material slab. One of the authors (M. C. K. W.) is supported by the EC Information Societies Technology (IST) program Development and Analysis of Left-Handed Materials (DALHM), Project No. IST-2001-35511. Another author (E. S.) acknowledges financial support by the Emmy-Noether Program of the German Research Council.

- ¹R. E. Collin, *Field Theory of Guided Waves* (Oxford University Press, Oxford, 1991).
- ²J. B. Pendry, A. J. Holden, W. J. Stewart, and I. Youngs, *Phys. Rev. Lett.* **76**, 4773 (1996).
- ³J. B. Pendry, A. J. Holden, D. J. Robbins, and W. J. Stewart, *IEEE Trans. Microwave Theory Tech.* **47**, 2075 (1999).
- ⁴V. G. Veselago, *Sov. Phys. Usp.* **10**, 509 (1968).
- ⁵R. A. Shelby, D. R. Smith, and S. Schultz, *Science* **292**, 77 (2001).
- ⁶M. C. K. Wiltshire, J. B. Pendry, I. R. Young, D. J. Larkman, D. J. Gilderdale, and J. V. Hajnal, *Science* **291**, 849 (2001).
- ⁷M. C. K. Wiltshire, J. V. Hajnal, J. B. Pendry, D. J. Edwards, and C. J. Stevens, *Opt. Express* **11**, 709 (2003).
- ⁸E. Shamonina, V. A. Kalinin, K. H. Ringhofer, and L. Solymar, *Electron. Lett.* **38**, 371 (2002).
- ⁹E. Shamonina, V. A. Kalinin, K. H. Ringhofer, and L. Solymar, *J. Appl. Phys.* **92**, 6252 (2002).
- ¹⁰M. C. K. Wiltshire, E. Shamonina, I. R. Young, and L. Solymar, *Electron. Lett.* **39**, 215 (2003).
- ¹¹F. W. Grover, *Inductance Calculations: Working Formulas and Tables* (Instrument Society of America, Research Triangle Park, N.C., 1981).
- ¹²Nippon Steel Chemical Co. Ltd., Advanced Material Division, 7-21-11, Nishi Gotanda, Shinagawa-ku, Tokyo 141-0031, Japan.